

## Complementarity of Particles and Pits in Freeze-Fractured Hepatic and Cardiac Gap Junctions

Ann M.G.L. De Mazière, Dietrich W. Scheuermann, and Philip A.P.M. Aertgeerts  
Institute of Histology and Microscopic Anatomy, University of Antwerp, B-2020 Antwerp, Belgium

**Summary.** Particles and pits of freeze-fractured gap junctions are considered as complementary structures despite the frequent observations of more regular and closer spacings of pits, ascribed to plastic deformation of particle arrays. Recently, however, the noncomplementarity of pits and particles in Purkinje fibers has been reported. To ascertain the relationship between both structures, gap junctions from fixed, cryoprotected liver and myocardium were investigated using spacing and density measurements and complementary replicas.

In hepatocyte gap junctions, the center-to-center distances (mean  $\pm$  SD) among pits,  $9.57 \pm 1.49$  nm, and particles,  $9.70 \pm 1.77$  nm, are not significantly different. Density determinations yielded a slightly higher value for the pits,  $(11,510 \pm 830)/\mu\text{m}^2$ , than for the particles,  $(11,230 \pm 950)/\mu\text{m}^2$ . In the myocardium, the spacing of the regularly arrayed pits,  $9.55 \pm 1.33$  nm, barely exceeds the value of  $9.44 \pm 1.62$  nm for the particles, which show some clustering. However, the packing density for the pits,  $(10,090 \pm 740)/\mu\text{m}^2$ , appears a little higher than that of the particles,  $(9,890 \pm 920)/\mu\text{m}^2$ . As density and spacing measurements provided no decisive answers, the positions of individual pits and particles of complementary junctional faces were recorded on transparent sheets and compared. In this fashion, a one-to-one correspondence between particles and pits could be established, while small discrepancies may be attributed to plastic deformation. Moreover, the collinearity of pits and particles may be suggested by the observation of a platinum grain in the center of many pits.

**Key Words** gap junctions · complementary replicas · plastic deformation · freeze-fracture · intramembranous particles · liver · myocardium

### Introduction

Gap junctions consist of patches of closely packed particles or connexons (Goodenough, 1975), spanning the membranes of contiguous cells and the intervening 2 nm gap and providing pathways for the direct intercellular exchange of ions and small molecules in the vast majority of animal tissues (Peracchia, 1980; Loewenstein, 1981). Each particle is composed of six identical, nonglycosylated protein

monomers (Makowski et al., 1977; Revel, Nicholson & Yancey, 1984), enclosing a morphologically distinct, hydrophilic channel (Hertzberg & Gilula, 1979; Zampighi, Corless & Robertson, 1980; Fujimoto, Ogawa & Ogawa, 1984).

Since Chalcraft and Bullivant (1970) and Steere and Sommer (1972) have demonstrated that, in complementary replicas of freeze-fractured hepatic and cardiac gap junctions, respectively, patches of particles on the protoplasmic face (PF) correspond to patches of pits on the exoplasmic face (EF), the individual particles and pits have been considered as complementary structures. In this view, the small dimple often observed in the top of the particles suggests the location of the central pore. Thus, it was assumed that the connexons, firmly attached to the inner half-membrane, are pulled through the outer half-membrane, leaving a complementary array of holes. As a consequence, the parameter most frequently investigated for the connexon packing is the center-to-center distance among particles rather than pits, since the latter are not consistently obvious in all freeze-fracture preparations due to local replication conditions and condensation of traces of residual vapor.

However, the observed small-scale mismatching between PF and EF, and the more regular arrangement of the pits, were related to fracturing and replica preparation artifacts (Chalcraft & Bullivant, 1970; Steere & Sommer, 1972; Caspar et al., 1977; Peracchia, 1977). Moreover, analyses of center-to-center distances among particles and pits in gap junctions of heart muscle and pancreatic acini consistently revealed about 1 nm lower values for the pits than for the particles, a discrepancy attributed to plastic deformation preferentially affecting the particles (Baldwin, 1979; Page & Upshaw-Earley, 1980; Délèze & Hervé, 1983; Meda et al., 1983; Page, Karrison & Upshaw-Earley, 1983; Scheuermann et al., 1984).

Instead, upon examination of PF-EF transitions in liver gap junctions, Goodenough and Revel (1970) questioned the collinearity of pits and particles. Recently, Kordylewski and Page (1985), establishing a ratio of 1.3–1.5 for the number of pits relative to the number of particles in complementary gap junctions, reported the noncomplementarity of pits and particles in cardiac Purkinje fibers.

Therefore, the relationship between gap junctional pits and particles in fixed, cryoprotected tissue has been reinvestigated, so as to ascertain the qualitative and quantitative interpretation of images of conventionally freeze-fractured gap junctions. In view of the distinct differences in the biochemical composition and immunological characteristics (Dermietzel et al., 1984; Nicholson et al., 1985), and in the structural organization (Shibata, Manjunath & Page, 1985) of hepatic and cardiac gap junctions, a quantitative analysis of gap junctions from both tissues has been performed, relying on measurements of center-to-center distance and packing density and on examination of complementary replicas.

## Material and Methods

### TISSUE PREPARATION AND FREEZE FRACTURE

After decapitation, a small wedge of tissue was rapidly excised from the left lateral liver lobe of young male Wistar rats, cut into small blocks and placed in a cold fixative containing 2% glutaraldehyde, 1.5% paraformaldehyde, 1.8 mM  $\text{CaCl}_2 \cdot 2\text{H}_2\text{O}$  and 0.1 M Na-cacodylate, at pH 7.4. To study cardiac gap junctions, ventricular myocardium of isolated, perfused rat hearts was used, as these preparations allow further investigations of the connexon configuration in relation to perfusion solutions of different composition. Therefore, male rats weighing 200–300 g were injected intraperitoneally with 2000 I.U. heparin, 1 hr before being stunned by a blow on the head and excision of the heart. After a few seconds in ice-cold modified Krebs-Henseleit (KH) bicarbonate buffer containing (in mM) 118 NaCl, 4.7 KCl, 2.5  $\text{CaCl}_2 \cdot 2\text{H}_2\text{O}$ , 1.2  $\text{MgSO}_4$ , 1.2  $\text{KH}_2\text{PO}_4$ , 25  $\text{NaHCO}_3$ , 11 glucose, at pH 7.4, the hearts were perfused for 20 min through a Langendorff cannula at a minimum flow rate of  $6 \text{ ml} \cdot \text{min}^{-1} \cdot \text{g}^{-1}$  heart wet wt with the KH solution at 37°C, continuously bubbled with  $\text{O}_2/\text{CO}_2$  (95:5). This equilibration time was chosen in order to allow recovery from initial enzyme release and to achieve a stable heart rate and coronary flow, while ultrastructural integrity was confirmed by electron microscopy of thin sections. After the stabilization period, perfusion was continued with a similarly oxygenated fixative consisting of 2% glutaraldehyde, 2.5 mM  $\text{CaCl}_2 \cdot 2\text{H}_2\text{O}$ , 0.1 M Na-cacodylate, pH 7.4, at 37°C for 10 min. Small tissue blocks from the middle portion of the left ventricular wall were immersed in fixative initially at 37°C and stored at 4°C for another 50 min.

For freeze fracture, specimens were incubated for 30 min, first in 10% and then 20% glycerol, followed by 1–4 hr in 30% glycerol, all in 0.1 M Na-cacodylate. The tissue blocks were then mounted on gold specimen carriers with a 1-mm central hole,

designed for a hinged double replica device. In some of the cylindrical pieces, a shallow longitudinal groove was made to facilitate recognition of complementary replica areas afterwards.

After freezing in nitrogen slush, the samples were freeze-fractured using a Balzers BAF 300 apparatus, equipped with electron beam guns and a quartz crystal thin film monitor, at  $-140^\circ\text{C}$  and less than  $8 \cdot 10^{-7}$  Torr. By starting the evaporation before fracturing, the fracture faces were replicated unidirectionally without delay with 2 nm of platinum/carbon at an angle of  $45^\circ$ , with an additional backing of 25 nm of carbon. Replicas were cleansed according to an improved method (De Mazière, Aertgeerts & Scheuermann, 1985), in order to ensure a high yield of intact complementary replicas. In brief, the replicated tissue was thawed in melting methanol, left for 1–3 days in liquid methanol in closed plastic containers at room temperature and digested in half-strength bleach with 5% ethanol. After subsequently cleansing in full-strength bleach and 50% saturated NaOH, the replicas were rinsed in double-distilled water and picked up on Formvar-coated 50-mesh grids with an asymmetric central mark.

### ELECTRON MICROSCOPY

Replicas were examined in a Siemens Elmiskop IA or 102 at 80 kV. On pairs of intact replicas with a slightly asymmetric shape, complementary areas were retrieved with the help of ground plans outlined on tracing paper. Gap junctions, lying in a plane perpendicular to the electron beam, as judged by sight, were photographed at an initial magnification of  $40,000 \times$ . On complementary replicas, both faces of each gap junction were photographed immediately one after another at  $40,000$  or  $80,000 \times$ . The microscopic magnifications were standardized with a micrograph of carbon grating with 2,160 lines/mm at the start of each session and by minimizing hysteresis effects in the lenses prior to each exposure.

### QUANTITATIVE ANALYSIS

For liver and heart muscle, respectively, 46 and 70 gap junctional aggregates from both fracture faces, distributed over several replicas from three organs, were analyzed. (i) *Center-to-center distances between particles and pits*: The electron micrograph sheets were projected by an Epidiascope Vh 2 (Leitz, Wetzlar, FRG) operating in the diascope mode, to a final magnification of  $240,000 \times$  onto a MOP AMO2 (Kontron, Eching, FRG) digitizing tablet. In each gap junction, 30 center-to-center distances between particles or pits and all their neighbors were measured along a line extending from the periphery to the center of the aggregate. Distances between adjacent particles with confluent shadowing metal caps were also included in the data files. To distinguish neighboring pits or particles from the more remote ones, the "obtuse angle criterion" (Page et al., 1983) was applied: after connecting all centers of pits or particles by lines, two particles or pits are no longer considered as neighbors if the interconnecting line is opposite to an obtuse angle formed by nearby lines. No measurements were made across the aisles in cardiac gap junctions. (ii) *Packing density*: In a similar manner, micrographs of 47 hepatic and 74 cardiac gap junctions were projected onto millimetric paper and the numbers of pits or particles counted within a square of 2 by 2 cm. Per gap junction, three squares were sampled, covering the zones where center-to-center spacings were measured.

Micrographs of 18 pairs of complementary gap junctional faces consisting solely of either pits or particles were printed to a final magnification of  $400,000\times$ . On transparent overlays, all centers of pits and particles on the complementary faces were independently marked with dots, allowing a comparison of their numbers and positions. The areas of complementary aggregates were determined by means of a digitizing tablet.

Results are expressed as mean values  $\pm$  SD, with  $n$  representing the sample size.

The equality of the variances of the samples to be compared was tested by means of the  $F$  test at the  $2P = 0.05$  level of significance. Comparison of quantitative data was accomplished by a  $t$  test or, in case of different variances, by a  $t'$  test. Values for the area of complementary gap junctional faces were matched by means of Wilcoxon's signed rank test. In order to estimate the relationship between center-to-center distance and density, Pearson's product-moment correlation coefficient was calculated.

## Results

### HEPATOCTE GAP JUNCTIONS

Gap junctions on the lateral hepatocyte membranes from fixed liver tissue consist of aggregates of pits or particles, or both, with a large variation in size and shape. Within the gap junctional aggregates, both particles and pits show a homogeneous, close packing, yet without any apparent regularity. Only now and then, this dense aggregation pattern is interrupted by round or oval open spaces, bearing a few nonjunctional particles. Occasionally, small junctional areas where the pits or particles are loosely arranged can be observed on dome-shaped elevations or slight depressions of the membrane.

As a first test for the one-to-one relationship of fixed, cryoprotected hepatocyte gap junctional particles and pits, their center-to-center distance and packing density were analyzed, considering only junctional areas with a typical dense packing.

Center-to-center distance measurements were made on 26 PF particle aggregates and 20 EF pit aggregates, including six pairs of complementary gap junctional faces (Fig. 1). After pooling all values for EF and PF, respectively, no significant difference ( $0.10 < 2P < 0.20$ ) could be demonstrated between the center-to-center spacing of the particles, i.e.,  $9.70 \pm 1.77$  nm ( $n = 786$ ), and the spacing of the pits, i.e.,  $9.57 \pm 1.49$  nm ( $n = 603$ ). Although not particularly noticeable at first sight, a more regular spacing of the pits in comparison to the particle spacing is reflected by the significantly smaller variance for the distances measured on the EF.

Next, as a measure for the packing pattern over a longer range, the densities of pits and particles were compared by means of three independent counts on 27 particle and 20 pit aggregates, includ-

**Table.** Junctional area and total number of particles and pits in complementary faces of liver and cardiac gap junctions

	PF area ( $\mu\text{m}^2$ )	Number of particles	EF area ( $\mu\text{m}^2$ )	Number of pits
Liver	0.16605		0.16986	
	0.03970	500	0.03953	497
	0.05017		0.04849	
	0.00494		0.00486	
	0.00372	60	0.00354	60
	0.00067		0.00064	
	0.02733	327	0.02765	326
Myocardium	0.00696	91	0.00646	93
	0.09919	1167	0.10479	1172
	0.03864	448	0.03729	448

ing those used for the center-to-center distance measurements (Fig. 1). For the packing on the PF, a mean density of  $11,230 \pm 950$  particles/ $\mu\text{m}^2$  ( $n = 81$ ) was found, whereas for the EF, a slightly larger value of  $11,510 \pm 830$  pits/ $\mu\text{m}^2$  ( $n = 60$ ) was obtained, with  $0.05 < 2P < 0.10$ . As indicated by the product-moment correlation coefficients of 0.55 and 0.54 for PF and EF, respectively, there appeared to be only a poor correlation between the mean center-to-center distance of each gap junction and the average of the three density determinations on each gap junction; instead, an inverse relationship between the density and the squared center-to-center distance had been expected.

Thus, in order to obtain a decisive answer, the numbers, positions and packings of particles and pits on seven pairs of complementary gap junctional faces (Fig. 2) have been compared, as well as the area occupied by the aggregates (Table).

First, center-to-center distance measurements on six pairs of complementary aggregates revealed a mean spacing for the particles, i.e.,  $9.50 \pm 1.84$  nm ( $n = 180$ ), identical to that for the pits, i.e.,  $9.50 \pm 1.51$  nm ( $n = 182$ ). Again, the smaller standard deviation for the pits points to a more regular arrangement in the EF aggregates. Secondly, the slightly higher mean density of the pits ( $11,210 \pm 650$ )/ $\mu\text{m}^2$  ( $n = 18$ ) did not differ significantly ( $0.10 < 2P < 0.20$ ) from the mean value for the particles, ( $10,890 \pm 760$ )/ $\mu\text{m}^2$  ( $n = 18$ ). Next, the area of seven pairs of level, complementary gap junctional faces was measured planimetrically, after tracing their outline through the centers of the peripheral pits or particles (Table). According to Wilcoxon's signed rank test for paired observations, there is no difference in the areas occupied by the pits and particles of one and the same gap junction.

Finally, for seven pairs of complementary gap

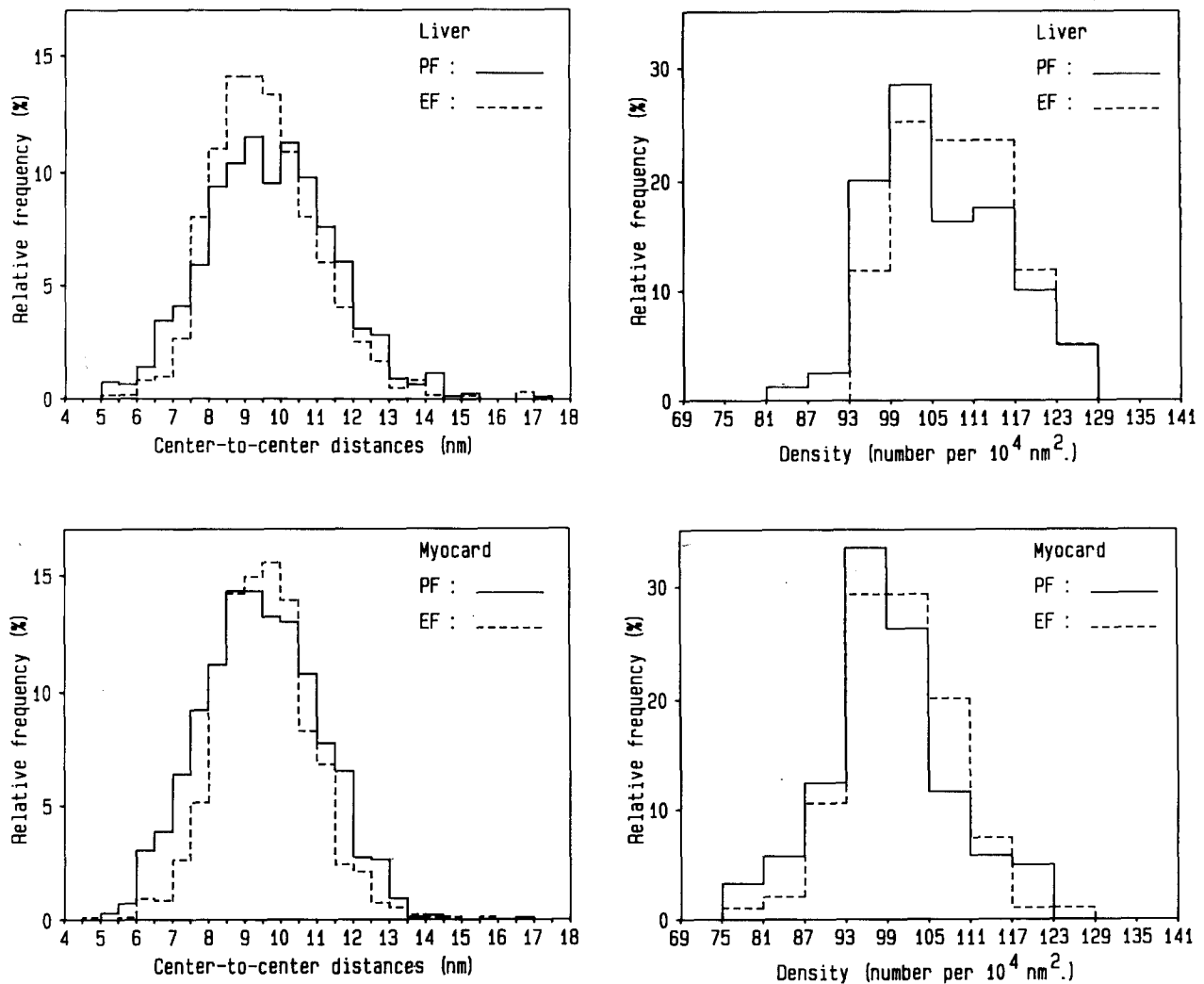


**Fig. 1.** Percentage histograms comparing packing characteristics of PF particles and EF pits in gap junctions from liver parenchyma and ventricular myocardium

junctional faces, all centers of particles and pits were recorded on transparent sheets superimposed on micrographs of one of both gap junctional faces, and this configuration of dots was fitted to the micrograph of the complementary face. From Fig. 2, it is clear that each dot, representing a particle on the PF, corresponds to one pit on the EF and vice versa. In the Table, the numbers of pits and particles counted on corresponding faces are listed. It is thus concluded that there exists a one-to-one relationship between the pits and particles of freeze-fractured fixed and cryoprotected hepatocyte gap junctions. Upon close inspection, small shifts of particles with respect to their corresponding pit occur in different directions among neighboring pairs of particles and pits.

The exact position of the pits with respect to the

center of the particles cannot be derived with certainty. Indeed, the gap junctional elements themselves provide the most accurate means of correlating complementary images. However, in the center of pits of favorably shadowed gap junctions, often a black dot of deposited metal is observed (Fig. 3). Either this platinum grain may represent the shadowing metal cap of a minute steep elevation at the bottom of the pit, in which case this elevation, or stub, could be part of the content of the central connexon pore, left in the center of the pit. Otherwise, the observed platinum grain could indicate a nucleation site. In aggregates of pits shadowed under higher angles, black dots are not visible since platinum grains, either shadowing an elevation or decorating a specific site, would be hidden in the shadowing metal patch partially filling the pit.

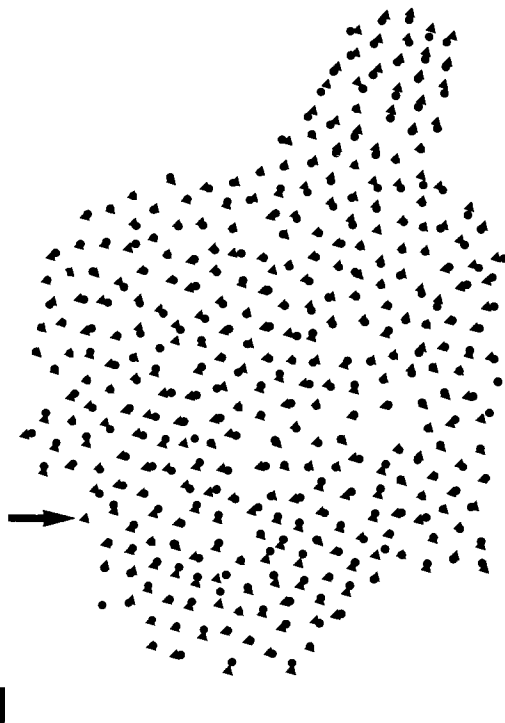
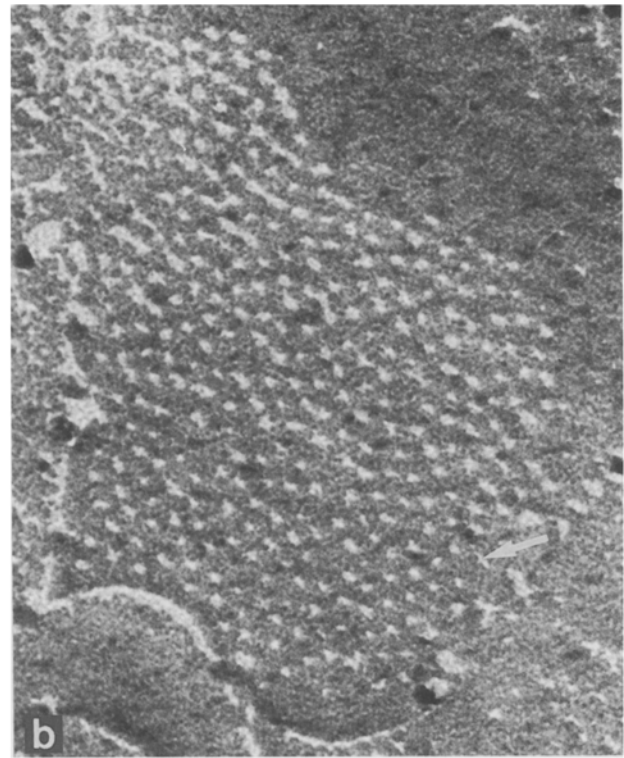
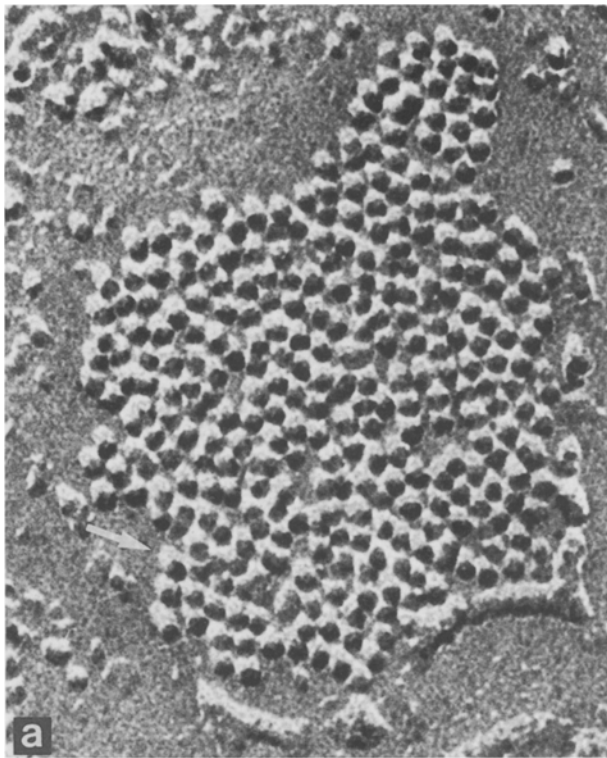


**Fig. 2.** Complementary configurations of hepatic tight and gap junction. 324,000 $\times$ . (a) PF; (b) EF; (c) matched configurations of particles (●) and pits (▲). The arrows point to a position where a particle, opposite to a pit, is lacking

pits are closely and rather orderly arrayed in small criss-cross oriented domains separated by smooth zones or aisles. On the PF, several particles tend to cluster, as indicated by coalescent metal caps, so that the disturbed order underlines the different appearance of PF and EF.

Center-to-center distance measurements on 38 PF and 32 EF aggregates (Fig. 1) revealed a mean spacing of  $9.44 \pm 1.62$  nm ( $n = 1,163$ ) for the particles, as compared with a slightly higher value of  $9.55 \pm 1.30$  nm ( $n = 969$ ) for the pits, with  $0.05 < 2P < 0.10$ . The significantly lower variance confirms the higher degree of order in the EF aggregates.

On the other hand, determinations of the packing density of 42 PF and 32 EF gap junctional faces, including those used for center-to-center measurements, yielded a slightly higher value,  $(10,090 \pm 740)/\mu\text{m}^2$  ( $n = 96$ ) for the pits, than for the particles, i.e.,  $(9,890 \pm 920)/\mu\text{m}^2$  ( $n = 126$ ), with  $0.05 < 2P < 0.10$  (Fig. 1).

As for the hepatocyte gap junctions, measurements of the former two parameters allow no definitive conclusions, but necessitate a comparison of

#### CARDIAC GAP JUNCTIONS

In perfusion-fixed, cryoprotected ventricular heart muscle, gap junctional particles and, in particular,

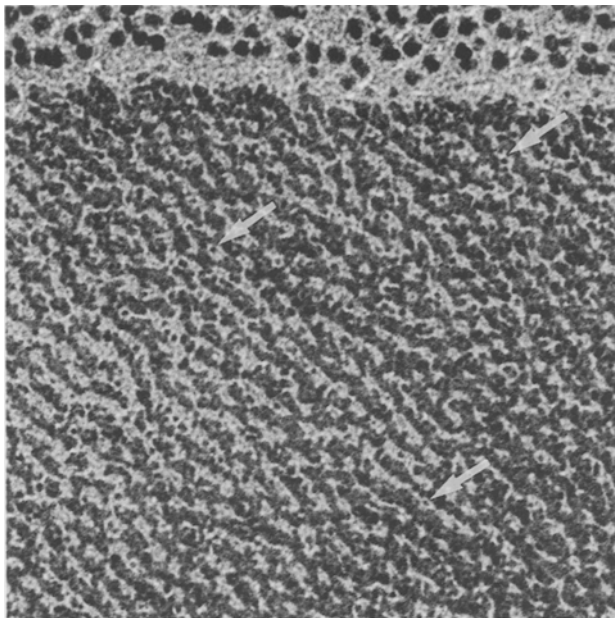


**Fig. 3.** Electron micrograph of freeze-fractured liver gap junction. Black dots (arrows) in the center of pits may represent part of the channel content. 411,000 $\times$

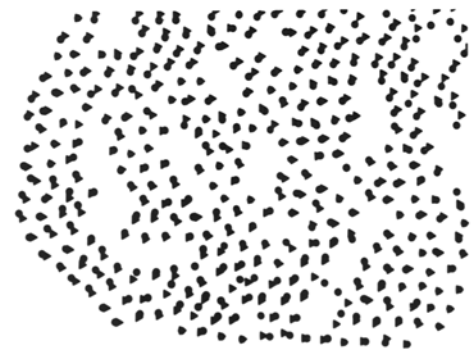
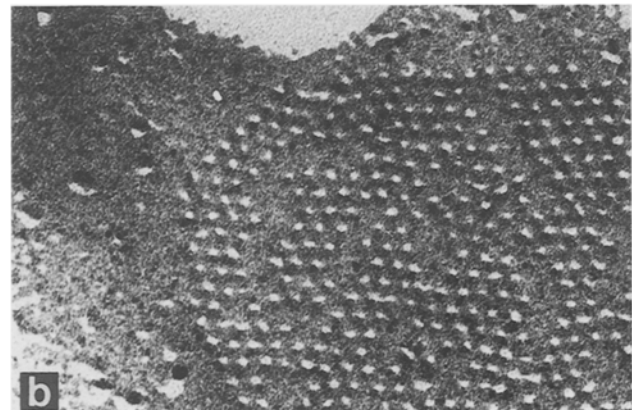
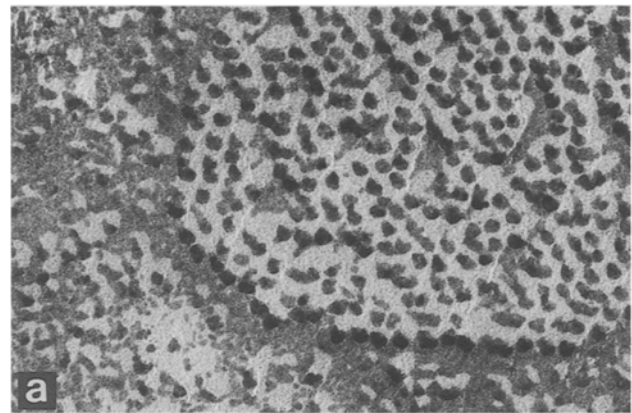
complementary gap junctional faces (Fig. 4 and Table). After recording all particles and pits of 11 pairs of complementary gap junctional aggregates on transparent sheets, each particle embedded in the PF appears obviously related to one pit in the EF (Fig. 4), with the corresponding EF and PF aggregates covering equal areas (Table). The few slight mismatches between the complementary configurations (Fig. 4c) are apparently due to shifts of particles with respect to the corresponding pit, in various directions. Analogous to the hepatocyte gap junctions, pits with a black dot in their center are observed in several EF aggregates.

### Discussion

By systematic comparison of complementary gap junctional faces, this study provides evidence for the one-to-one correspondence between gap junctional particles and pits in glutaraldehyde-fixed and cryoprotected liver parenchyma and myocardium of the rat.

An examination of complementary replicas was needed in order to establish the one-to-one relationship between individual pits and particles from one and the same gap junction, since center-to-center distance and density measurements failed to yield any unambiguous answers.

Among the factors contributing to the subtle



**C**

**Fig. 4.** Complementary configurations of a cardiac gap junction. 291,000 $\times$ . (a) PF; (b) EF; (c) matched configurations of particles (●) and pits (▲)

differences in measuring results for PF and EF, several sources of error or variation are equally applicable to measurements made on PF and EF, and, by ideal random sampling, will therefore cancel each other out. First, the dimensions of the gap junctional faces and the spacings of particles and pits may be distorted to some extent by strains imposed on the replica during preparation or by unrecognized tilting of replica parts with respect to the hori-

zontal plane in the electron microscope. Deviations from the horizontal plane, however, may be more conspicuous on one or the other face, depending on the local shadowing angle or on the aspect of the contrasted particulate PF in comparison to the relatively even EF. A correction for such errors could be introduced by tilting the replicas with a goniometer stage in the microscope. Second, the existing large variation in packing characteristics within a tissue, a single replica, or even within one gap junction (Page et al., 1983), leads to a considerable uncertainty in assessing possible small differences in spacing.

On the contrary, some types of errors are specific for one or the other junctional face. The observed tendency towards higher packing densities on complementary as well as noncomplementary pitted gap junctional faces may be promoted by the very nature of the objects. On the one hand, the particles are accentuated by replication and thus clearly visualized. However, in some positions they may be clustered so tightly that their shadowed areas coalesce. In this study, such large indented metal caps have been interpreted as being composed of several clumped particles, as has been justified by images of rotary shadowed, glutaraldehyde-fixed gap junctions of the liver (Sikerwar & Malhotra, 1981). Nevertheless, erroneous interpretation of the tightest clumps may entail an underestimation of the true particle number. On the other hand, the dimensions of the pits are decreased by partial filling-up during shadowing, reducing their perception, but showing them more clearly spaced. Occasionally, small gaps in the platinum film could mistakenly be counted as pits. Furthermore, as is apparent from the smaller variance for the center-to-center spacing on the EF, the pits display a more regular arrangement than the particles, enhancing the different aspect of both aggregates, each implying specific difficulties in counting densities and measuring distances.

Although in previous studies on hepatocyte gap junctions no extensive quantitative comparison of the packing of pits and particles has been performed, the range of center-to-center distances was mentioned as being similar for pits and particles (Chalcroft & Bullivant, 1970; Goodenough & Revel, 1970; Peracchia, 1977; Caspar et al., 1977). On the other hand, in mammalian cardiac muscle, the observation of about 1 nm lower values for the spacing of pits as compared with that of the particles (Baldwin, 1979; Page & Upshaw-Earley, 1980; Délèze & Hervé, 1983; Page et al., 1983; Scheuermann et al., 1984) has led to the complementarity of these structures being questioned (Kordylewski & Page, 1985). It seems likely that the observed difference

between the mean center-to-center distances of particles and pits is partly dependent on the degree to which distances between clustered particles are included in the measurements. Whereas Délèze and Hervé (1983) and Scheuermann et al. (1984) also included clumped particles in the measurements, Baldwin (1979) considered only clearly resolved particles. In the present analysis, which aims at a comparison with the spacing of pits, the observer's bias towards clearly separated particles was minimized by measuring distances between 6-8 systematically sampled particles per junction and all their neighbors, whether clustered or not. Furthermore, assuming a regular array of connexons in the undisturbed cardiac gap junctions—as suggested by the pattern of the pits—the clustering of some of the particles during preparative manipulations simultaneously causes the distance between the neighboring particles to increase. However, if by particle clustering at the edges of the hexagonally packed domains a minute broadening of the aisles occurs, then the shortening of distances between clustered particles is not compensated for, since no measurements are performed over the aisles. Subscribing to previous studies, the present results again stress the need for precisely defined measuring conditions for center-to-center spacing analyses.

While recording the position of pits and particles on transparent sheets laid over complementary gap junctional faces, particles with confluent metal caps were also marked. Minor differences in the numbers of pits and particles counted on complementary junctional faces may therefore arise partly from misinterpretation of such particle clumps. Otherwise, in some rare cases, a particle may have been lost during fracturing, leaving no trace but the pit on the EF. Apart from these minimal discordancies, the superposition of the independently recorded configurations strikingly shows the one-to-one correspondence of particles and pits, which is in sharp contrast to the results of Kordylewski and Page (1985), who used comparable approaches and found 1.3-1.5 times more pits than particles. However, these investigators used sheep cardiac Purkinje strands, which may contain gap junctions with different properties. In addition, prior to a comparable fixation and cryoprotection, the ventricular myocardium used in the present study has been perfused *in vitro* under standardized conditions. An alteration of the fracturing behavior of the gap junctions by these manipulations is possible, though improbable, since stable, regularly beating heart preparations have been achieved. Furthermore, the discrepancy between our results and those of Kordylewski and Page (1985) may be due to different interpretations of clumped particles. In



order to avoid misinterpretation of particle clumps, the latter investigators compared rotary shadowed EFs and PFs of the same gap junction, but not on complementary replicas. Therefore, variability in packing pattern within a single gap junction may have contributed to the observed difference in density. A final possible explanation for the frequently established higher density of the pits is that curved gap junctions may be preferentially fractured through the membrane with the smallest curvature, so that the particles on the outside bend PF are spread over a larger surface than the pits. Slightly curved gap junctional faces could then have been included inadvertently in quantitative analyses. A clue for this explanation lies in the observation that the so-called satellite gap junctions in cardiac muscle (Page et al., 1983; Green & Severs, 1984) always appear with a concave PF or a convex EF.

Although in the present study the one-to-one relationship of individual pits and particles is clearly demonstrated, small shifts in different directions of some pits with respect to the corresponding particles are apparent. These small misfits may have arisen partly from cumulated errors in placing the dots on the two transparent sheets, but, in view of the one-to-one correspondence of particles and pits, they are bound to result mainly from distortions of one or both configurations during fracturing or irradiation. Since it is hardly probable that the highly ordered arrays of pits have been produced by any distortion, it appears likely that the clustering of particles, for which there is no counterpart on the EF, is an artifact of the applied technique. As it was shown that the energy released during fracturing may cause a temperature rise of 50–70°C (Grujters & Bullivant, 1986), plastic deformation or lateral dislocations of particles in the softened lipid matrix may have occurred (Sleytr & Robards, 1977; Gross, Bas & Moor, 1978). The susceptibility of gap junctional particles to such distortions has been demonstrated in freeze-fractured, deep-etched liver gap junctions, split by hypertonic saline, where fracture faces with disorderly particle arrays may be observed beside hexagonally ordered connexon lattices on the external surface of the same gap junction (Hirokawa & Heuser, 1982).

Previously the position of pits and particles on the same axis was questioned by Goodenough and Revel (1970) for hepatocyte gap junctions and recently by Kordylewski and Page (1985) in cardiac Purkinje fibers. On our micrographs, the platinum grain often observed in the center of pits, both from hepatic and cardiac gap junctions, may represent either the shadowing metal cap of a minute stub or a nucleation site on the bottom of the pit. In the former case, the platinum grain may have portrayed

part of the connexon pore content, which would then be complementary to the dimple in many particles. In this fashion, the grains might indicate a col-linear position of particles and pits. Alternatively, the platinum grain may have decorated a site with particular physico-chemical properties. In view of indications that platinum may decorate hydrophilic sites, the observed nucleation site, again, could correspond to the aqueous connexon channel. In this case, the hydrophilic properties of this site could be assessed by controlled decoration with ice crystal-lites (Gross & Moor, 1978). In order to distinguish between shadowing and decoration phenomena, which occur simultaneously in conventionally cast replicas, decoration should be inhibited during shadowing or the specimens should be decorated with platinum at an elevation angle of 90°, so as to avoid shadowing (Winkler, Wildhaber & Gross, 1985). However, these procedures are hampered by the unevenness of the fracture plane. Otherwise, a clue for the position of the pits relative to the particles might come from superimposition of stereoimages.

In conclusion, the present study confirms the current structural concept of the gap junction and its behavior during fracturing analogous to other intramembranous particles such as (Na<sup>+</sup>,K<sup>+</sup>)-ATPase (Ting-Beall, Burgess & Robertson, 1986). By the demonstration of the one-to-one correspondence of the gap junctional pits and particles, the acquisition of quantitative data on the distribution of connexons over the cell surface, from measurements on the PF as well as on the EF of glutaraldehyde-fixed liver and ventricular myocardium, is justified. Although particle and pit configurations in liver parenchyma and myocardium are qualitatively similar in replicas of fixed, cryoprotected and unfixed, shock-frozen tissue (Raviola, Goodenough & Raviola, 1980; Sikerwar & Malhotra, 1981; Severs, 1985; Aertgeerts, De Mazière & Scheuermann, 1986), an identical fracturing behavior of connexons after quick freezing remains to be confirmed. Furthermore, plastic deformation may be an important factor in limiting the accuracy of center-to-center distance measurements if structural alterations concomitant to functional changes are to be established. Thus, in order to increase the reliability of quantitative descriptions of connexon packing patterns, arrays of pits should be analyzed instead of particles, to avoid the effects of secondary particle clustering. Alternatively, in order to minimize distortions, quick freezing, as by the method of Heuser, Reese and Landis (1976), followed by freeze fracturing near liquid helium temperatures, as already suggested by Hanna et al. (1981), will probably provide the most valuable information



on the actual arrangement of gap junctional connexons.

## References

- Aertgeerts, P., De Mazière, A.M.G.L., Scheuermann, D.W. 1986. Gap junctional reorganization in hypoxic rat heart. *Verh. Anat. Ges.* **80**:541–542
- Baldwin, K.M. 1979. Cardiac gap junction configuration after an uncoupling treatment as a function of time. *J. Cell. Biol.* **82**:66–75
- Caspar, D.L.D., Goodenough, D.A., Makowski, L., Phillips, W.C. 1977. Gap junction structures. I. Correlated electron microscopy and X-ray diffraction. *J. Cell Biol.* **74**:605–628
- Chalcroft, J.P., Bullivant, S. 1970. An interpretation of liver cell membrane and junction structure based on observation of freeze-fracture replicas of both sides of the fracture. *J. Cell Biol.* **47**:49–60
- Délèze, J., Hervé, J.C. 1983. Effect of several uncouplers of cell-to-cell communication on gap junction morphology in mammalian heart. *J. Membrane Biol.* **74**:203–215
- De Mazière, A.M.G.L., Aertgeerts, P., Scheuermann, D.W. 1985. A modified cleansing procedure to obtain large freeze-fracture replicas. *J. Microsc. (Oxford)* **137**:185–188
- Dermietzel, R., Leibstein, A., Frixen, U., Janssen-Timmen, U., Traub, O., Willecke, K. 1984. Gap junctions in several tissues share antigenic determinants with liver gap junctions. *EMBO J.* **3**:2261–2270
- Fujimoto, K., Ogawa, K.S., Ogawa, K. 1984. Direct visualization of the hydrophilic channel in the gap junction under an electron microscope using alkali-metal ions. *Acta Histochem. Cytochem.* **17**:453–456
- Goodenough, D.A. 1975. Methods for the isolation and structural characterization of hepatocyte gap junctions. In: *Methods in Membrane Biology*. E.D. Korn, editor. Vol. 3, pp. 51–80. Plenum, New York
- Goodenough, D.A., Revel, J.P. 1970. A fine structural analysis of intercellular junctions in the mouse liver. *J. Cell Biol.* **45**:272–290
- Green, C.R., Severs, N.J. 1984. Gap junction connexon configuration in rapidly frozen myocardium and isolated intercalated disks. *J. Cell Biol.* **99**:453–463
- Gross, H., Bas, E., Moor, H. 1978. Freeze-fracturing in ultra-high vacuum at  $-196^{\circ}\text{C}$ . *J. Cell Biol.* **76**:712–728
- Gross, H., Moor, H. 1978. Decoration of specific sites on freeze-fractured membranes. In: *Electron Microscopy 1978*. J.M. Sturgess, editor. Vol. 2, pp. 140–141. Microscopical Society of Canada, Toronto
- Gruijters, W.T.M., Bullivant, S. 1986. Freeze-fracturing at defined temperatures provides information on temperature rise during fracture, and on membrane complementarity. *J. Microsc. (Oxford)* **141**:291–301
- Hanna, R.B., Reese, T.S., Ornberg, R.L., Spray, D.C., Bennett, M.V.L. 1981. Fresh frozen gap junctions: Resolution of structural detail in the coupled and uncoupled states. *J. Cell Biol.* **91**:125a
- Hertzberg, E.L., Gilula, N.B. 1979. Isolation and characterization of gap junctions from rat liver. *J. Biol. Chem.* **254**:2138–2147
- Heuser, J.E., Reese, T.S., Landis, D.M.D. 1976. Preservation of synaptic structure by rapid freezing. *Cold Spring Harbor Symp. Quant. Biol.* **40**:17–24
- Hirokawa, N., Heuser, J. 1982. The inside and outside of gap-junction membranes visualized by deep etching. *Cell* **30**:395–406
- Kordylewski, L., Page, E. 1985. Are gap junctional pits and particles complementary structures? *Biophys. J.* **47**:506a
- Loewenstein, W.R. 1981. Junctional intercellular communication: The cell-to-cell membrane channel. *Physiol. Rev.* **61**:829–913
- Makowski, L., Caspar, D.L.D., Phillips, W.C., Goodenough, D.A. 1977. Gap junction structures. II. Analysis of the X-ray diffraction data. *J. Cell Biol.* **74**:629–645
- Meda, P., Findlay, I., Kolod, E., Orci, L., Petersen, O.H. 1983. Short and reversible uncoupling evokes little change in the gap junctions of pancreatic acinar cells. *J. Ultrastruct. Res.* **83**:69–84
- Nicholson, B.J., Gros, D.B., Kent, S.B.H., Hood, L.E., Revel, J.-P. 1985. The  $M_r$  28,000 gap junction proteins from rat heart and liver are different but related. *J. Biol. Chem.* **260**:6514–6517
- Page, E., Karrison, T., Upshaw-Earley, J. 1983. Freeze-fractured cardiac gap junctions: Structural analysis by three methods. *Am. J. Physiol.* **244**:H525–H539
- Page, E., Upshaw-Earley, J. 1980. Gap junctional particle distributions in rat ventricle. *Fed. Proc.* **39**:298
- Peracchia, C. 1977. Gap junctions: Structural changes after uncoupling procedures. *J. Cell Biol.* **72**:628–641
- Peracchia, C. 1980. Structural correlates of gap junction permeation. *Int. Rev. Cytol.* **66**:81–146
- Raviola, E., Goodenough, D.A., Raviola, G. 1980. Structure of rapidly frozen gap junctions. *J. Cell Biol.* **87**:273–279
- Revel, J.-P., Nicholson, B.J., Yancey, S.B. 1984. Molecular organization of gap junctions. *Fed. Proc.* **43**:2672–2677
- Scheuermann, D.W., De Mazière, A., De Groot-Lasseel, M.H.A., Aertgeerts, P. 1984. Cardiac gap junction configuration after ischemia. *Verh. Anat. Ges.* **78**:183–184
- Severs, N.J. 1985. Intercellular junctions and the cardiac intercalated disk. In: *Advances in Myocardiology*. P. Harris and P.A. Poole-Wilson, editors. Vol. 5, pp. 223–242. Plenum, New York
- Shibata, Y., Manjunath, C.K., Page, E. 1985. Differences between cytoplasmic surfaces of deep-etched heart and liver gap junctions. *Am. J. Physiol.* **249**:H690–H693
- Sikerwar, S., Malhotra, S. 1981. Structural correlates of glutaraldehyde induced uncoupling in mouse liver gap junctions. *Eur. J. Cell Biol.* **25**:319–323
- Sleytr, U.B., Robards, A.W. 1977. Plastic deformation during freeze-cleavage: A review. *J. Microsc. (Oxford)* **110**:1–25
- Steere, R.L., Sommer, J.R. 1972. Stereo ultrastructure of nexus faces exposed by freeze-fracturing. *J. Microsc. (Paris)* **15**:205–218
- Ting-Beall, H.P., Burgess, F.M., Robertson, J.D. 1986. Particles and pits matched in native membranes. *J. Microsc. (Oxford)* **142**:311–316
- Winkler, H., Wildhaber, I., Gross, H. 1985. Decoration effects on the surface of a regular protein layer. *Ultramicroscopy* **16**:331–339
- Zampighi, G., Corless, J.M., Robertson, J.D. 1980. On gap junction structure. *J. Cell Biol.* **86**:190–198

Received 28 October 1986; revised 11 March 1987